

Electrochemical behaviour of silver and rhenium electrodes in molten alkali fluorides

ABED M. AFFOUNE^{1,*}, ABDELKADER SAILA¹, JACQUES BOUTEILLON² and JEAN C. POIGNET²

¹Laboratoire LAIGM, Département de Chimie Industrielle, Université de Guelma, BP 401 24000, Guelma, Algeria

²LEPMI, UMR 5631 INPG-CNRS associé à UJF, ENSEEG, Domaine Universitaire, BP 75 38402, Saint Martin d'Hères, France

(*author for correspondence, fax: + 213-3720-7268, e-mail: affoune2@yahoo.fr)

Received 14 February 2006; accepted in revised form 21 August 2006

Key words: rhenium, silver, semi-integration, simulation, voltammetry

Abstract

Electrochemical oxidation of silver and rhenium electrodes in molten LiF–NaF–KF eutectic at 600 °C was investigated by cyclic and convolutional voltammetry. Simulated Cyclic voltammograms were calculated to reinforce understanding of the reaction mechanism. A theoretical relationship was proposed to determine standard potentials from voltammograms of metallic electrodes having an oxidation process governed by Butler–Volmer kinetics. The reversibility of silver oxidation was established and the number of exchanged electrons and the standard potential of the Ag/Ag(I) couple were determined. The rhenium electrode oxidation process was shown to be quasi-reversible and the Re/Re(x) standard potential was estimated.

1. Introduction

The electrodeposition of refractory metals is often carried out using the molten eutectic LiF–NaF–KF solvent because of its large electrochemical window, which is limited cathodically by the reduction of potassium ions and anodically by the oxidation of metals used as working electrode [1]. Many authors have been interested in the oxidation of metallic electrodes either to study the thermodynamics or the kinetics of the process or to generate an *in situ* redox couple for use as an internal reference system. In fused LiF–NaF–KF eutectic, the anodic behaviour of copper, iron and nickel electrodes has been studied by several authors [2–4] using cyclic and convolutional voltammetry. In molten NaCl–KCl the anodic oxidation of platinum was investigated by cyclic voltammetry [5]. Later, the electrochemical behaviour of sodium, nickel, molybdenum and iron in molten NaF was studied using convolutional voltammetry and galvanostatic pulses [6]. A silver electrode is often used as working electrode for electrochemical studies in molten salts [7, 8].

In previous work, we studied the electrochemical reduction of KReO₄ [7, 9] solutions. The reduction of perrhenate ions occurred in two steps corresponding respectively to the exchange of one and two electrons and both yielding soluble species. The first step was assumed to be reversible and the second irreversible. We suggested that metallic rhenium was produced by

disproportionation of a soluble species. Solutions of rhenium hexafluoride were cathodically reduced via a single irreversible charge transfer step.

In this investigation we studied the anodic dissolution of rhenium metal in molten LiF–NaF–KF eutectic at 600 °C. Cyclic voltammograms were calculated and we used the silver system, which is reversible, as a model system to validate the simulation. We were interested in the determination of the corresponding rhenium standard potential and of the number of electrons exchanged by the anodic reaction. We developed a theoretical relationship for the determination of the standard potential of Me/Me(X) couples from voltammetric curves.

2. Experimental

The measurements were carried out in an airtight stainless steel cell. The electrolyte was the eutectic mixture LiF–NaF–KF (46.5–11.5–42 mol%). It was introduced to a graphite crucible placed in the cell and purified as described previously [7]. A three electrode-system was used. The working electrode was either a silver wire or a rhenium wire of, 1 and 0.5 mm diameter, respectively. The counter electrode was the graphite crucible and a platinum wire was used as a comparison electrode. All potentials were referred to the equilibrium potential of the K/K⁺ couple corresponding to the cathodic limit of the solvent.

3. Results and discussion

3.1. Phenomenological analysis

The reduction of potassium ions and the oxidation of fluoride ions limit the theoretical potential range of the LiF–NaF–KF eutectic. Hence, the width of the potential range, calculated from the free enthalpy of formation of KF at 600 °C [10] is 4.96 V. Typical voltammograms, obtained on silver and rhenium electrodes, are shown in Figure 1. The anodic dissolution potential sampled at 10 mA cm⁻² is 2.76 V on silver and 2.74 V on rhenium. These values represent the effective experimental electrochemical window of the solvent, which is narrower than the theoretical (4.96 V), because the anodic limit is in fact due to oxidation of the metallic electrodes. Comparison with the values obtained under the same conditions on iron ($E = 1.36$ V) [4], nickel ($E = 1.85$ V) [4] and copper ($E = 2.28$ V) [2], indicates that silver and rhenium are the most noble materials in this media.

The shapes of the anodic parts of the voltammograms of Figure 1 are markedly different. Five simulated voltammograms corresponding to various values of the electron transfer kinetic parameters are presented in Figure 2. The calculation was based on general Butler–Volmer kinetics and the Nicholson and Shain technique [11, 12], as indicated in Appendix A. Calculated voltammograms showed that a decrease in reversibility leads to a shift of the reverse cathodic peak towards negative potentials. The degree of reversibility increases when the dimensionless kinetic constant $\omega = (\pi n F v / RT D_M^{n+})^{1/2} / k^0$, decreases. The experimental curves show the reversible character of the silver electrode and indicate the irreversibility of the rhenium system.

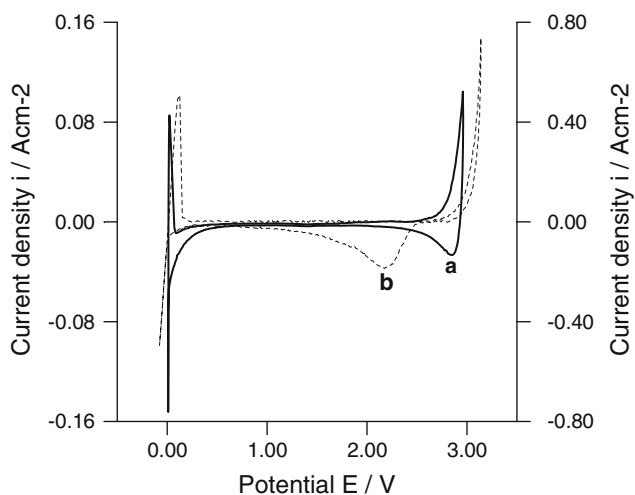


Fig. 1. Voltammograms obtained on silver (a) and rhenium (b) electrodes in the molten LiF–NaF–KF eutectic, $T = 600$ °C, $v = 0.5$ V s⁻¹ (on silver), $v = 1$ V s⁻¹ (on rhenium).

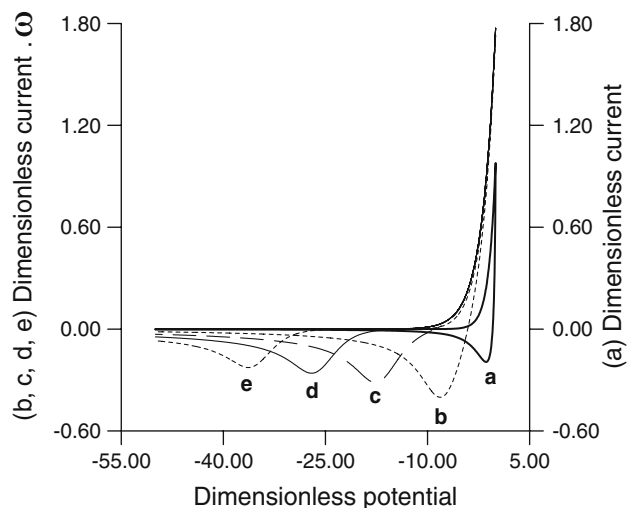


Fig. 2. Theoretical cyclic voltammograms obtained for different dimensionless kinetic constant $\omega = (\pi n F v / RT D_M^{n+})^{1/2} / k$, cathodic charge transfer coefficient $\alpha = 0.5$, anodic charge transfer coefficient $\beta = 0.5$ (a) $\omega = 0$; (b) $\omega = 10^2$; (c) $\omega = 10^4$; (d) $\omega = 10^6$; (e) $\omega = 10^8$.

3.2. Silver oxidation

3.2.1. LSV analysis

Some studies, related to the establishment and analysis of theoretical voltammograms of reversible insoluble-soluble systems $M \rightleftharpoons M^{n+} + ne$, have been published [13–15]. Teherani et al. [15] have shown that for a reversible M/M^{n+} system, the anodic oxidation voltammograms verify the following characteristics:

$$dE/d \ln(I) = RT/nF \quad (1)$$

$$E_{I=0} - E_p = 0.96 RT/nF \quad (2)$$

$$E_\lambda - E_{I=0} = 0.409 RT/nF \quad (3)$$

$$I_p/I_\lambda = -0.196 \quad (4)$$

where E = electrode potential, E_λ = switching potential (the potential at time λ corresponding to the instant of the reverse of potential scan from anodic scan to cathodic scan), $E_{I=0}$ = potential at zero current, E_p = cathodic peak potential, I = current, I_p = cathodic peak current, I_λ = current at switching potential.

In such conditions, the number of electrons exchanged, n , can therefore be calculated from relations 1, 2 or 3. Furthermore, to estimate the standard potential, Berghoute et al. [5] derived the following equation:

$$E^0 = E - (RT/nF) \ln((i/(nF))^{3/2} (RT/v D_M^{n+})^{1/2}) \quad (5)$$

where i is the current density and v is the scan rate.

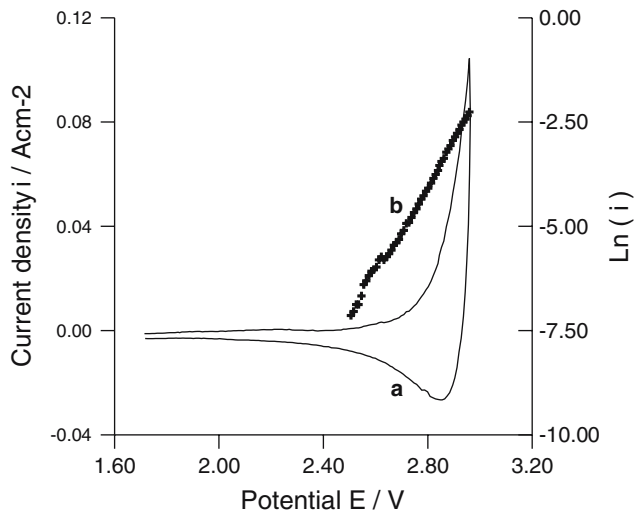


Fig. 3. (a) Voltammogram obtained on silver electrode in the anodic limit region deduced from Figure 1(a). (b) Logarithmic analysis of the current density related to the forward part of voltammogram (a).

The anodic part of a voltammogram related to the oxidation of a silver electrode is shown in Figure 3 together with its logarithmic analysis. The shape of the voltammogram, especially the position of the cathodic peak which is very close to the oxidation potential of silver, indicates that the Ag/Ag(I) couple is reversible. Furthermore the theoretical values of $dE/d\ln(I)$ and $E_{I=0} - E_p$, (Equations (1) and (2)) are close to the experimental ones deduced from Figure 3, reported in Table 1. These results show that the number of electrons exchanged is one. The difference between theoretical and experimental values can be attributed to the ohmic drop. E^0_{Ag/Ag^+} was calculated using Equation (5). The value $10^{Ag/Ag^+} \text{ cm}^2 \text{ s}^{-1}$ for $D_{(Ag)}^+$ was used in the calculation in the absence of published data, considering the experimental value $D_{(Ag)}^+ = 1.0 \times 10^{-5} \text{ cm}^2 \text{ s}^{-1}$ in molten eutectic LiCl-KCl at the same temperature [16]. The application of relation (5) to different sets of values (E, i), obtained from the forward part of the voltammogram in Figure 3, yields the value $E^0 = 3.617 \pm 0.002 \text{ V}$ taking $n = 1$ (Table 2).

Table 1. Comparison between theoretical values calculated from the relations (1) and (2), and experimental values obtained from Figure 3

Relationship	Theoretical value	Experimental value	Number of electrons, n
$dE/d\ln(I)$	$0.075/n$	0.089	0.84
$E_{I=0} - E_p$	$0.072/n$	0.082	0.88

Table 2. Standard potential calculated from relation (5) for different sets of values (E, i) obtained from the forward part of voltammogram in Figure 3

$E, \text{ V}$	2.839	2.871	2.896
$i/\text{A cm}^{-2}$	25.71×10^{-3}	39.84×10^{-3}	52.78×10^{-3}
$E^0/\text{V} (n = 1)$	3.616	3.615	3.619

3.2.2. Semi-integral analysis

To overcome the effect of ohmic drop other authors [4, 6] used the semi-integration technique or convoluted voltammetry [17–19] for the estimation of n and E^0 . In the case of the oxidation of an insoluble species to a soluble species with diffusion-controlled mass transfer, the surface concentration of the oxidized species $C_M^{n+}(0, t)$ is linked to the semi-integral of the current, m , by

$$C_M^{n+}(0, t) = +m/nF\sqrt{D_M^n} \quad (6)$$

If the process is reversible, with the initial concentration $C_M^{n+} = 0$, the Nernst equation becomes:

$$E = E^0 - (RT/nF) \ln(nF\sqrt{D_M^n}) + (RT/nF) \ln(m) \quad (7)$$

This expression shows that the forward and backward convoluted curves are superposed. Their logarithmic analysis yields the determination of the number of exchanged electrons n . Provided that D_M^{n+} is known, the standard potential E^0 can also be determined.

We used the algorithm developed by Oldham [20] to obtain the semi-integral curves and the corresponding logarithmic analysis. The convoluted voltammogram of Figure 3 and its logarithmic analysis are reported in Figure 4. The good superposition of forward and backward curves demonstrates the reversibility of the electron exchange. The slope of the logarithmic plot yields the numerical value $n = 0.9$.

Taking n as equal to unity, Equation (7) yields:

$$E^0 = E_{(m=1)} + (RT/F) \ln(F\sqrt{D_M^{n+}}) \quad (8)$$

Considering the experimental value of E extrapolated to $m = 1$ (Figure 4), $E_{(m=1)} = 3.218 \text{ V}$, gives:

$$E^0 = 4.079 + 0.0375 \ln(D_{Ag^+}^+) \quad (9)$$

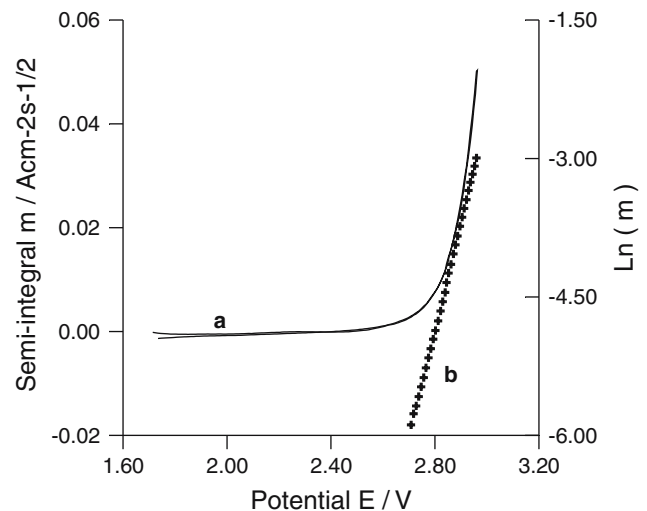


Fig. 4. (a) Semi-integral of voltammogram represented in Figure 3(b) Logarithmic analysis related to the forward part of semi-integral (a).

Thus, taking D_{Ag^+} as equal to $10^{-5} \text{ cm}^2 \text{ s}^{-1}$ yields the value $E^0 = 3.647 \text{ V}$

3.2.3. Simulation of the voltammograms

Experimental results obtained by semi-integration and LSV are almost similar. Nevertheless, the numerical values of n , E^0 , D , used for the simulation were those obtained from the convoluted curves, which can be corrected for the effect of ohmic drop. A satisfactory match of the experimental and simulated curves is obtained. The effect of the arbitrary choice of $D = 10^{-5} \text{ cm}^2 \text{ s}^{-1}$ on the match of experimental and simulated curves was analysed through the effect of the value of E^0 . It was observed that a slight change in the values of E^0 by $+13 \text{ mV}$ ($E^0 = 3.660 \text{ V}$) or -16 mV ($E^0 = 3.631 \text{ V}$) gave the best match of the experimental and simulated curves. The experimental and simulated curves corresponding to $E^0 = 3.631 \text{ V}$ are shown in Figure 5.

3.3. Rhenium oxidation

3.3.1. Theoretical study

In the case of a quasi-reversible electron exchange process controlled by diffusion, the following relation can be obtained from the Butler–Volmer equation [21]:

$$E = E^0 + (RT/((\alpha + \beta)nF)) \ln(C_O(0, t)/C_R(0, t)) \quad (10)$$

where E is the electrode potential along the linear sweep voltammetry curve, and with α is the cathodic charge transfer coefficient, β the anodic charge transfer coefficient, $C_O(0, t)$ the surface concentration of oxidized

species, $C_R(0, t)$ the surface concentration of reduced species.

As far as the oxidation of a metal is concerned the surface concentration of the oxidized species $C_M^{n+}(0, t)$ and the semi-integral of the current, m , are linked by Equation (10). Thus Equation (10) becomes:

$$E = E^0 + (RT/((\alpha + \beta)nF)) \ln(m/(nF\sqrt{D_M^{n+}})) \quad (11)$$

The potential at zero current along the reverse potential scan, $E_{I=0}$, is given by

$$E_{I=0} = E^0 + (RT/((\alpha + \beta)nF)) \ln(m_{I=0}/(nF\sqrt{D_M^{n+}})) \quad (12)$$

with $m_{I=0}$ the semi-integral at zero current.

Table 3 shows the details of calculation around the zero current point ($E_{I=0}$, $I = 0$) using a calculated voltammogram obtained with these different parameters:

$$\omega = 10^6, \alpha = 0.35, \beta = 0.25, n = 2, E^0 = 2.70 \text{ V}, D = 1.0 \times 10^{-5} \text{ cm}^2 \text{ s}^{-1}, T = 873 \text{ K}, \nu = 0.5 \text{ V s}^{-1}.$$

Table 3 shows that Equation (7), related to the reversible system, gives a value of $E^0 = 2.44 \text{ V}$, which is very different from the value of 2.70 V used for calculation. However, Equation (12) gives the accurate value. Consequently, we consider that only Equation (12) can be used to calculate standard potential for quasi-reversible metallic systems.

3.3.2. Determination of the standard electrode potential of the Re/Re(X) couple

The direct and reverse anodic part of the voltammogram presented in Figure 1b are shown in Figure 6, together with their semi-integral analysis, while a Tafel representation of the polarization curve is shown in Figure 7. The large hysteresis observed between the direct and reverse scans of the semi-integral curves shown the irreversibility of the electron exchange process. This result allows the determination of the Re/Re(x) standard electrode potential using relation (12). The values $E_{I=0} = 2.657 \text{ V}$ and $m_{I=0} = 0.177 \text{ A cm}^{-2} \text{ s}^{-1/2}$ are picked up from the curves in Figure 6, while the slopes of the Tafel plots (Figure 7) are used to determine the values of αn and βn :

$$\alpha n = 1.93 \pm 0.10$$

$$\beta n = 0.74 \pm 0.05$$

Since literature values for diffusion of rhenium species in the molten LiF–NaF–KF eutectic only concern Re(VI) ($D_{\text{Re(VI)}} = 0.8 \times 10^{-5} \text{ cm}^2 \text{ s}^{-1}$ at $600 \text{ }^\circ\text{C}$ [9], the latter species is first considered, the number of electron exchanged is assumed to be 6. The application of Equation (12) using the set of values given in this section for $E_{I=0}$, $m_{I=0}$, αn , βn , $D_{\text{Re(x)}}$, and n , yields $E^0 = 2.914 \text{ V}$.

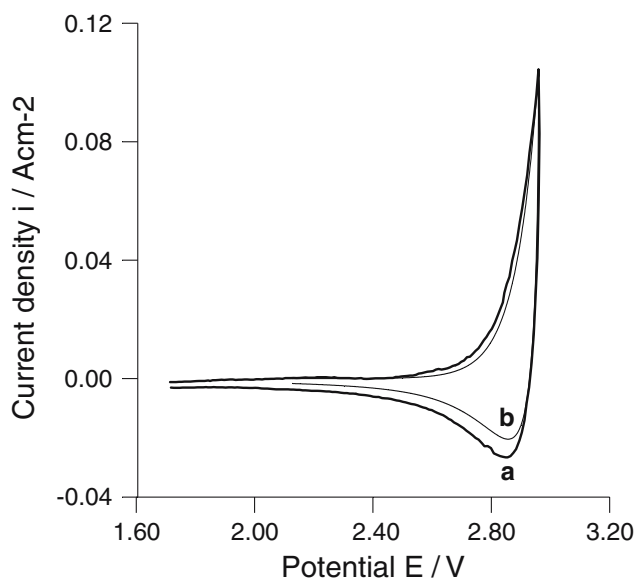


Fig. 5. (a) Experimental voltammogram obtained on silver electrode; $T = 873.15 \text{ K}$, $\nu = 0.5 \text{ V s}^{-1}$. (b) Theoretical voltammogram calculated with the following parameters: $n = 1$, $E^0 = 3.631 \text{ V}$, $T = 873.15 \text{ K}$, $\nu = 0.5 \text{ V s}^{-1}$.

Table 3. Values of current density (i), semi-integral of current density (m) and standard potential (E^0) in the potential region (E) of zero current point

E/V	$i/A\text{ cm}^{-2}$	$m/A\text{ cm}^{-2}\text{ s}^{-1/2}$	E^0_7/V	E^0_{12}/V
2.079487	3.190369E-6	2.264709E-2	2.463194	2.718998
2.077607	2.873121E-6	2.262473E-2	2.461351	2.717180
2.075726	2.558324E-6	2.260244E-2	2.459507	2.715361
2.073846	2.245902E-6	2.258022E-2	2.457664	2.713543
2.071966	1.935775E-6	2.255806E-2	2.455821	2.711724
2.070085	1.627868E-6	2.253597E-2	2.453977	2.709905
2.068205	1.322105E-6	2.251395E-2	2.452134	2.708086
2.066325	1.018411E-6	2.249199E-2	2.45029	2.706267
2.064444	7.167106E-7	2.247009E-2	2.448446	2.704447
2.062564	4.169322E-7	2.244827E-2	2.446602	2.702628
2.060684	1.190026E-7	0.0224265	2.444759	2.700809
2.058803	-1.771496E-7	0.0224048	2.442914	2.698989
2.056923	-4.715954E-7	2.238317E-2	2.441071	2.697169
2.055043	-7.644049E-7	0.0223616	2.439227	2.695349
2.053162	-1.055647E-6	2.234009E-2	2.437382	2.693529
2.051282	-1.345392E-6	2.231864E-2	2.435538	2.691709
2.049401	-1.633706E-6	2.229726E-2	2.433693	2.689888
2.047521	-1.920657E-6	2.227594E-2	2.431849	2.688068
2.045641	-2.206311E-6	2.225468E-2	2.430005	2.686248
2.043760	-2.490735E-6	2.223348E-2	2.42816	2.684427
2.041880	-2.773994E-6	2.221235E-2	2.426316	2.682606
2.040000	-3.056153E-6	2.219127E-2	2.424471	2.680786

E^0_7 and E^0_{12} are the standard potentials calculated by Equations (7) and (12) respectively.

An error as large as $\Delta E^0 = 0.04\text{ V}$ on the value of the $\text{Re}/\text{Re}(x)$ standard electrode potential can be estimated from the uncertainty of the n and $D_{\text{Re}(x)}$ values used in the calculation, and also from the error in the determination of αn .

4. Conclusion

The electrochemical behaviour of silver and rhenium electrodes in molten LiF-NaF-KF at $600\text{ }^\circ\text{C}$ was studied by cyclic and convolutional voltammetry. The results confirmed that the kinetics of the silver anodic

oxidation is a reversible process. The calculated number of electrons exchanged, n , and the standard potential E^0 of the silver couple were $n = 1$ and $E^0 = 4.079 + 0.0375 \ln(D)\text{ V}/(\text{K}/\text{K}^+)$.

In the case of the rhenium electrode the anodic oxidation process was shown to be governed by Butler-Volmer kinetics. An equation for the calculation of the standard potential for such systems was derived and applied to estimate the standard potential of the rhenium couple, $E^0 = 2.914 \pm 0.04\text{ V}/(\text{K}/\text{K}^+)$.

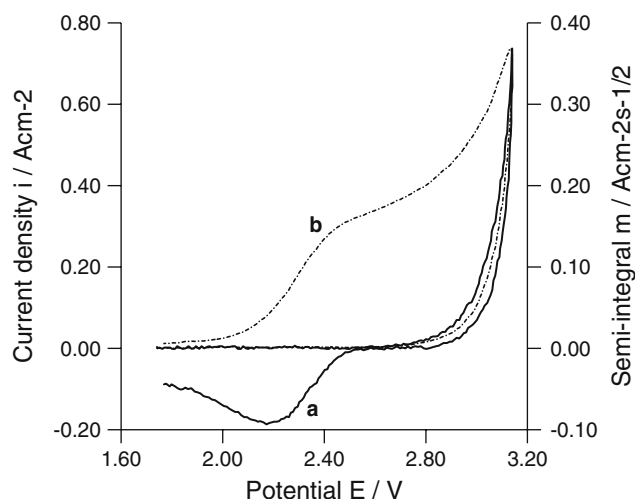


Fig. 6. (a) Voltammogram obtained on rhenium electrode in the anodic limit region deduced from Figure 1(a). (b) Semi-integral analysis.

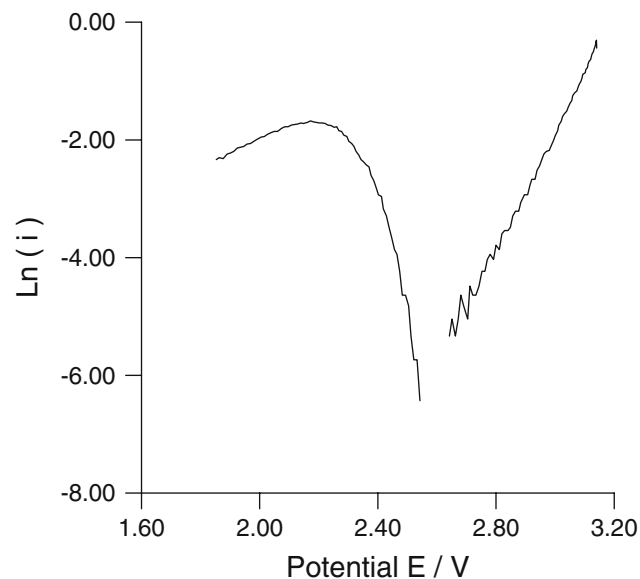
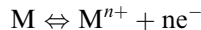


Fig. 7. Logarithmic analysis of the current density related to the voltammogram of rhenium presented in Figure 6(a).

Appendix A

Metal dissolution under quasi-reversible charge transfer process can be represented by the equation:



The current change is given by Butler–Volmer equation:

$$I(t) = nFAk \left[C_M(0, t) \cdot \exp\left\{\frac{\beta nF[E - E^0]}{RT}\right\} - C_{M^{n+}}(0, t) \cdot \exp\left\{\frac{[-\alpha nF][E - E^0]}{RT}\right\} \right] \quad (A1)$$

C_M and $C_{M^{n+}}$ are respectively the concentration of the metal and the corresponding cations. α and β are cathodic and anodic transfer coefficients respectively.

By assuming planar semi-infinite diffusion of the metallic cations, after solving Fick's second law, we set:

$$C_M^{n+}(0, t) = \frac{1}{nFA\sqrt{D_M^{n+}}} \cdot \frac{1}{\sqrt{\pi}} \int_0^t \frac{I(\tau)}{\sqrt{t - \tau}} \cdot d\tau \quad (A2)$$

For linear sweep voltammetry the electrode potential is given by

$$E = E_i + v \cdot t \quad \text{for first anodic scan, } 0 < t \leq \lambda \quad (A3)$$

$$E = E_i + 2v\lambda - v \cdot t \quad \text{for reversed cathodic scan, } t\lambda \quad (A4)$$

E_i is the initial potential while λ and v are respectively the reversal potential time and the scan rate.

By combination of Equations (2–4), we established the general equation for the current:

$$I(t) = nFA(\pi D)^{1/2} (nFv/RT)^{1/2} \psi(at) \quad (A5)$$

where $\psi(at)$ is given by the following integral:

$$\int_0^{at} \frac{\psi(Z)}{\sqrt{at - Z}} dZ = [\theta S(at)]^{(\alpha+\beta)} - \psi(at)\omega[\theta S(at)]^\beta \quad (A6)$$

with

$$\theta = \exp(nF/RT(E_i - E^0))$$

$$a = nFv/RT$$

$$S(t) = \exp(at) \quad \text{for } 0 < t \leq \lambda$$

$$S(t) = \exp(2a\lambda - at) \quad \text{for } t\lambda$$

$$\omega = \frac{\sqrt{\pi D_M^{n+} a}}{k^0}$$

We used the technique developed by Nicholson and Shain [11] to obtain numerical calculation of $\psi(at)$. The values of current can then be obtained for a given set of values of α , β , ω and switching potential E_λ . The voltammograms corresponding to different values of ω and consequently to different rate of charge transfer are presented in Figure 2.

References

1. J. De Lepinay and P. Paillere, *Electrochim. Acta* **29** (1984) 1243.
2. D. Renaud, *PhD thesis* INP Grenoble (1985).
3. H. Wendt, K. Reuhl and V. Schwarz, *Electrochim. Acta* **37** (1992) 237.
4. A. Robin and J. De Lepinay, *Electrochim. Acta* **37** (1992) 2433.
5. Y. Berghoute, A. Salmi and F. Lantelme, *J. Electroanal. Chem.* **365** (1994) 171.
6. N. Adhoun, J. Bouteillon, D. Dumas and J.C. Poignet, *J. Electroanal. Chem.* **391** (1995) 63.
7. A.M. Affoune, J. Bouteillon and J.C. Poignet, *J. Appl. Electrochem.* **25** (1995) 886.
8. R. Boen and J. Bouteillon, *J. Appl. Electrochem.* **13** (1983) 277.
9. A.M. Affoune, J. Bouteillon and J.C. Poignet, *J. Appl. Electrochem.* **32** (2002) 521.
10. JANAF, Thermochemical tables 2 edn., Nat. Stand. Ref. Data Serv., Nat. Bur. Standards (1976).
11. R.S. Nicholson and I. Shain, *Anal. Chem.* **36** (1964) 706.
12. S. Casadio, *J. Electroanal. Chem.* **72** (1976) 243.
13. Y. Kanzaki and S. Oayagui, *J. Electroanal. Chem.* **36** (1972) 297.
14. S. Casadio, *J. Electroanal. Chem.* **67** (1976) 123.
15. T. Teherani, K. Itaya and A.J. Bard, *Nouv. J. Chim.* **2** (1978) 481.
16. J.C. Poignet, *PhD thesis* INP Grenoble France (1972).
17. M. Goto and K.B. Oldham, *Anal. Chem.* **45** (1973) 2043.
18. J.C. Imbeaux and J.M. Saveant, *J. Electroanal. Chem.* **44** (1973) 169.
19. P.J. Mahon and K.B. Oldham, *J. Electroanal. Chem.* **464** (1999) 1.
20. K.B. Oldham, *J. Electroanal. Chem.* **112** (1981) 341.
21. A. J. Bard and L. R. Faulkner, 'Electrochemical Methods: Fundamentals and Applications', (John Wiley Sons, INC., New York, 2001) 110 pp.